UNIVERSITY OF CALIFORNIA
RIVERSIDE

Site-Targeted Biomimetic Nanoparticles for Local Suppression of Retinal Vascular Inflammation in Diabetes

A Thesis submitted in partial satisfaction
of the requirements for the degree of

Master of Science

in

Bioengineering

by

Neha R. Palegar

September 2018

Dissertation Committee:
Dr. Kaustabh Ghosh, Chairperson
Dr. Masaru Rao
Dr. Jin Nam

The Dissertation of Neha R. Palegar is approved:

_____

_____

_____

Committee Chairperson

University of California, Riverside

ACKNOWLEDGEMENTS

I would like to start by thanking my Professor Dr. Kaustabh Ghosh for giving me the opportunity to pursue my research in his lab. He has been an inspiration in many ways and has truly molded me into the researcher I am today.

I would also like to the acknowledge the immense contributions made towards my project by my fellow lab members Andrea Cabrera, Irene Santiago and Venkatesh Tavva. Their constant support and affection made my time in lab memorable

DEDICATION

I would like to dedicate this work to my family, without their love and encouragement this thesis would not have been possible

ABSTRACT OF THE THESIS

Site-Targeted Biomimetic Nanoparticles for Local Suppression of Retinal Vascular Inflammation in Diabetes

by

Neha R. Palegar

Master of Science, Graduate Program in Bioengineering
University of California, Riverside, September 2018
Dr. Kaustabh Ghosh, Chairperson

Retinal vascular inflammation is a common characteristic of diabetes. It is marked by upregulation of a major retinal endothelial cell adhesion molecule ICAM-1 that promotes leukocyte-endothelial adhesion. The adherent leukocytes subsequently release cytotoxic, hyperpermeability and pro-inflammatory factors to cause extensive vascular damage in the retina that often lead to diabetic retinopathy (DR), a vision-threatening condition that affects nearly 40% of all people with diabetes. Past studies have identified retinal endothelial ICAM-1 expression as a rate-limiting step in DR pathogenesis because inhibiting it blocked DR progression in vivo. A common anti-ICAM-1 therapy for DR involves the use of salicylates that block activation of NF-KB, a major transcription factor required for ICAM-1 upregulation. However, the clinically-used high levels of salicylates cause severe adverse off-target effects in the body. To address this major limitation, this

work describes the use of biomimetic nanoparticles (NPs) that selectively deliver salicylate to ICAM-1-expressing retinal endothelial cells (ECs) and blocks leukocyte-EC adhesion. Specifically, these biomimetic NPs are derived from red blood cell membranes, surface modified with an ICAM-1-targeting single chain variable fragment (scFv), and loaded with sodium salicylate. Detailed physicochemical characterization revealed that these NPs are ~160±35 nm in diameter, successfully conjugate anti-ICAM-1 scFv on their surface, and exhibit ~45% drug incorporation. Importantly, in vitro studies show that these drug-loaded NPs undergo preferential (~2-fold greater) uptake in ICAM-1-expressing retinal ECs and, crucially, exhibit a remarkable 700-fold greater efficacy of sodium salicylate in blocking leukocyte-EC adhesion. These promising findings lay the foundation for more detailed assessment of this anti-inflammatory nanotherapeutic as a new and improved treatment strategy for DR.

Table of Contents

TITLE PAGE I

ACKNOWLEDGEMENTS IV

DEDICATION V

ABSTRACT VI

LIST OF FIGURES IX

CHAPTER-1 1

- CHRONIC VASCULAR INFLAMMATION 1
- DIABETIC RETINOPATHY 2
- DIABETIC RETINOPATHY IS AN INFLAMMATION MEDIATED DISEASE 3
- SALICYLATES AS A POTENTIAL ANTI-INFLAMMATORY THERAPY FOR DIABETIC RETINOPATHY 4
- ADVANTAGES OF NANOTHERAPEUTICS 5
- BIOMIMETIC PARTICLES FOR LONG-CIRCULATING DRUG DELIVERY 6
- PROPOSED NANOTHERAPEUTIC APPROACH 7

CHAPTER-2 8

- INTRODUCTION 8
- MATERIALS AND METHODS 9
- RESULTS AND DISCUSSION 13
- CONCLUSIONS 23
- FIGURES 24

CHAPTER-3 34

- CONCLUSION AND FUTURE DIRECTIONS 34

REFERENCES: 37

List of Figures

Fig 1: Synthesis of Red Blood Cell derived ghost particles 24

Fig 2: Preparation of nanoparticles using sonication and extrusion.....25

Fig 3: Incorporation of synthetic lipids and the conjugation of scFv.....26

Fig 4: Loading sodium salicylate into RBC-NLs and the subsequent size characterization.....27

Fig 5: SDS-PAGE characterizing the protein make-up of the RBC ghost and RBC-NL membrane.....28

Fig 6: Size and Zeta potential values of the synthesized samples.....29

Fig 7: Uptake of RBC-NLs by Human Retinal Endothelial Cells.....30

Fig 8: Uptake of surface modified scFv conjugated RBC-NLs by Human Retinal Endothelial Cells.....31

Fig 9: Anti-Inflammatory effects of free sodium salicylate.....32

Fig 10: Monocyte-EC adhesion assay for the estimating drug efficacy of encapsulated drug.....33

List of Abbreviations

RBC-NL	Red Blood Cell Nanoliposome
scFv	single chain variable fragment
RBC-NL-scFv	Red Blood Cell Nanoliposome scFv
CAM	Cell adhesion molecules
DR	Diabetic retinopathy
DLS	Dynamic Light Scattering
EC	Endothelial cell
HREC	Human Retinal Endothelial Cell
ICAM-1	Intercellular cell adhesion molecule-1
Nf-kB	Nuclear factor kappa B
NL	Nanoliposome
TNF-α	Tumor necrosis factor-α

CHAPTER-1

INTRODUCTION

Chronic vascular inflammation

Vascular inflammation is marked by the expression of cell adhesion molecules on the surface of endothelial cells. The circulating leukocytes recognize and adhere to the cell surface glycoproteins which stabilizes the cell-cell interaction and also facilitates leukocyte transmigration to the site of injury. Under normal circumstances, the expression of pro-inflammatory factors subside overtime as the injury heals and the endothelium reverts back to its quiescent state. However, due to some abnormal conditions the process of inflammation never ceases, leading to chronic vascular inflammation. Hyperglycemia is one such disorder that supports a pro-inflammatory environment causing sustained activation of endothelial cells.

Diabetes is one of the most common metabolic disorders characterized by high blood glucose levels. This disorder is prevalent worldwide, affecting about 450 million people and projected to increase to approximately 700 million by the year 2045 [1]. There are two major types of diabetes, type I, an autoimmune disorder where the body's immune system destroys pancreatic B-cells resulting in insulin deficiency. While Type II is the more common form of diabetes, where hyperglycemia is a result of impaired insulin secretion and insulin resistance. It is known that high blood glucose levels affect the micro and/or macro vascular structures in various organs resulting in vascular complications. One such

major complication that involves vascular inflammation and damage in the retina is called Diabetic Retinopathy (DR).

Diabetic Retinopathy

It is estimated that about 191 million people will suffer with this disorder amongst which 56.3 million cases will be of vision threatening Diabetic Retinopathy by the year 2030 [2]. Diabetic retinopathy involves extensive damage to the small blood vessels and neurons of the retina. The stages of DR can be classified into 2 different categories, the early stage is non-proliferative (NPDR) marked by the appearance of microaneurysms, extensive damage to the retina and abnormalities of the microvascular structure and capillary nonperfusion [3]. In the proliferative stage of DR (PDR), capillary non-perfusion and degeneration of the vasculature leads to hypoxia conditions. This results in ischemia and eventually leads to neovascularization mediated by the secretion of Vascular Endothelial Growth Factor (VEGF) [4]. The blood-retinal barrier also loses its integrity becoming increasingly permeable to small as well as large molecules [5], this is consistent in early as well as the late stages of DR [3].

The current therapies for DR focus on the treatment of the disease in its advanced stages, once the disease has transitioned from NPDR to PDR. The therapies for DR include panretinal photocoagulation (PRP) that uses thermal burns throughout the retinal periphery to inhibit retinal neovascularization. This mode of treatment reduces rates of moderate vision loss in 50% of the patients suffering with advanced form of DR but, this causes loss of peripheral vision [6]. Vitreoretinal surgery is for non-clearing vitreous hemorrhage from

cases of PDR with tractional retinal detachment. But 20-30% of them experience severe vision loss after surgery. Intravitreal steroid injection is also effective but, it causes side effects such as cataract formation and glaucoma [7], [8]. Intravitreal anti-VEGF injections is the most effective therapy in treating DR with successful vision gain in patients suffering with DR for about 1 to 2 years [9]. But, this is difficult to administer in patients who cannot comply with regular check-up and injections. Also about 40-50 % people respond poorly to this treatment. Hence there is a need to develop better treatments for DR, and preferably those that can inhibit the progression at its early stage.

Diabetic Retinopathy is an inflammation mediated disease

The physiologic and morphological changes observed in the microvasculature of the eye in diabetic patients is linked to inflammation. Most of the early symptoms of DR which includes vascular leakage and capillary non-perfusion is attributed to the selective homing of leukocytes to retinal vessels [10]. Also, the continuous recruitment and subsequent adhesion of leukocytes (termed leukostasis) causes severe damage to the endothelial cells leading to the breakdown of blood-retinal barrier. Thus, linking retinal leukostasis spatially and temporally to the early symptoms of DR. ICAM-1 and CD18, which are the major inflammatory surface proteins expressed by activated endothelial cells facilitate this adhesion and extravasation of circulating leukocytes [10], [11], [12, p. 88]. After one month of inducing diabetes, mice showed increased levels of ICAM-1 mRNA levels. This coincided with the development of diabetic retinal leukostasis and breakdown of the blood-retinal barrier [11], [13]. Importantly, pharmacologic or genetic inhibition of ICAM-1 alone blocked the progression of DR, thus underscoring the crucial role of ICAM-1 in DR

pathogenesis [11], [10]. Mice models of DR also showed that ICAM-1 and CD18 are actively involved in the long-term development of retinal vascular lesions associated with DR [10] suggesting that inflammation continues to persist even in the later stages of the disease.

The expression of the surface proteins mediating inflammation is controlled at the level of gene transcription through the activation of pro-inflammatory transcription factors, like Nuclear Factor-kappa-B (NF-κβ). NF-κβ is secreted in the cytoplasm as a dimer in its inactive state. It is activated when the signal induced IκB protein kinase phosphorylates the two serine residues in the Iκβ regulatory domain, releasing the NF-κβ to migrate in to the nucleus to initiate the inflammatory process. Increasing evidence shows that NF-κβ activation plays a vital role in the early stages of Diabetic Retinopathy (DR). A variety of other transcription factors have also been speculated to have a role in inflammation but additional studies are still necessary to identify the roles of these transcription factors [14]. NF-κβ controls various inflammatory aspects of DR, they partly control the expression of ICAM-1 and other proteins like VCAM, alpha 4/CD49d that mediates leukocyte adhesion [15].

Salicylates as a potential anti-inflammatory therapy for Diabetic Retinopathy

As DR is an inflammatory disease, promising therapies for inflammation mediated vascular conditions would be the use of anti-inflammatory drugs that could inhibit or control the sustained activation of endothelial cells. Salicylates are one such commercially available

anti-inflammatory drugs that have previously been shown to cease the translocation of NF-KB into the nucleus by preventing the phosphorylation and degradation of the inhibitor Iκβ-α [16]. Salicylates are worth considering, as clinical trials and animal studies with rats have shown its effect on ceasing diabetes induced degeneration of retinal capillaries [17], [16]. Also, recent study shows that salicylates inhibited the progression and development of DR [18]. Clinical trials with humans showed decrease in microaneurysms, but these observations were not consistent. This could be attributed to the fact that insufficient dosage of salicylates was administered into the body to treat disease at its advances stages [18].

Advantages of Nanotherapeutics

Though salicylates are very effective as anti-inflammatory drugs, the treatment of chronic inflammation via systemic route requires high doses of salicylates to inhibit the TNF-α induced expression of E-selectin, VCAM-1 and ICAM-1, all of which are controlled by NF-κβ [16], [19]. But high doses of systematically administered salicylates have severe adverse side effects on various organs of the body, including the central nervous system, gastrointestinal tract as well as causing toxicity in the lungs and kidneys. The off-target interactions also leave a very small fraction of the administered drug in circulation, as a consequence, reduces the drug half-life drastically. This raises the need to develop a method to control the delivery and release of the drug and possibly restrict the release only at the site of interest.

It is well-known that nanotherapeutics has the potential to improve drug bioavailability, pharmacokinetics, efficacy and safety [20], [21]. Also, with the attachment of specific site targeting moieties, drug delivery can be restricted only to the desired target tissue, which is impossible to achieve by administering drugs via the conventional route [22]. In the past, artificially engineered nanoparticles have been designed for use in drug delivery. Rationale design, control and diversity of the materials provide a huge advantage in using these as drug carriers [23]. Amongst these, PEG conjugated liposomes are the best engineered long-circulating particles [24]. But the immune masking effect that PEG provides is transient and as a result PEGylated particles are eventually cleared by the circulating macrophages. The constant exposure to PEG particles also results in the production of Anti-PEG antibodies exacerbating clearance [25], [26]. This has been a major hindrance in utilizing the complete potential of nanoparticles in therapeutics and its subsequent translation to the clinic [27], [24].

Biomimetic particles for long-circulating drug delivery

Cell carriers have been gaining attention as potential long-circulating particles for drug delivery. Based on the application, targeted tissue and the property of the drug being incorporated, different carrier systems are usually considered. The most common amongst these include low density lipoproteins, natural peptides, viral vectors, cell and cell ghosts [28]. The various inherent properties allow these carries to carry out diverse set of functions within the body that is ideal for drug delivery vehicles. Lipid membrane encloses all the internal contents, polysaccharide components of these particles are involved in intracellular signal transduction and storage, proteins have structural and functional uses, they can be

the targeting moieties we need in drug delivery [28]. The many advantages like biodegradability, biocompatibility, non-toxicity and prolonged circulation times make these particles ideal for inflammation targeting [29].

Proposed nanotherapeutic approach

This work, proposes the synthesis of Red Blood Cell derived nanoparticles by preserving the *stealth* properties and further modify the surface to attach site targeting fragments. Since endothelial ICAM-1 is selectively upregulated at sites of chronic vascular inflammation, it presents a preferable molecular target for site targeting nanotherapeutic delivery. Hence, anti-ICAM IgGs can be tethered on the surface of the nanoparticles for targeting. But using the whole IgG would be problematic for two reasons, one, attaching an entire IgG molecule on the surface would make the nanoparticle very bulky, two, the F_c domain of the IgG would activate complement system resulting in rapid clearance from the body and nullify the advantage of tethering site targeting moieties on the surface [30]. To overcome this problem, only the variable fragment of the antibody that can preferentially bind to ICAM-1 expressing retinal endothelial cells is conjugated on the surface of the nanoparticle [31]. The RBC nanoparticles are loaded with sodium salicylate to inhibit the translocation of NF-κβ into the nucleus. As a result, treat the vascular complications that occurs due to diabetes. Preferential site-targeting combined with the endogenous nature of the nanoparticle should increase the circulation times of the drug carrier, reduce adverse off-target effects of the drugs and increase drug efficacy by several folds.

CHAPTER-2

Development of erythrocyte membrane derived site-targeting nanoparticles

Introduction

The innate properties of Red Blood Cells (RBCs) make them ideal drug carriers as the primary function of these cells is the delivery of "cargoes" within the body. These cells have long circulation periods and the entire inner volume along with its extended surface is available for drug loading. This makes them extremely attractive for intravascular drug delivery, as these characteristics of RBCs restricts unintended extravasation [32]. The major advantage in using these cells for drug delivery is their *stealth* property. The cell membrane has various "self-marker" proteins on their surface that help bypass the immune system [32], [33]. Amongst which, CD47 glycoprotein eludes phagocytosis through signaling with phagocyte receptor, SIRPα [34], [35]. As the RBC-membrane derived nanoparticles are synthesized from the blood sample of the patient, these particles can effectively evade clearance by the immune cells.

To further enhance the therapeutic efficacy, the RBC membrane can be modified to allow the attachment of with site-targeting moieties like, peptides, aptamers, antibodies and antibody fragments [36], [37].

As discussed in the previous chapter, retinal vascular inflammation is a common characteristic of diabetes. It is marked by upregulation of the major retinal endothelial inflammatory marker, ICAM-1. One of the vascular complications that is mediated by inflammation includes Diabetic Retinopathy (DR). Past studies have implicated ICAM-1 upregulation as the rate limiting step in DR pathogenesis. As a result, potential therapies

would include the use anti-inflammatory drugs that can particularly target ICAM-1, whose expression is in turn controlled by the nuclear factor NF-KB. Salicylates are the most commonly known anti-inflammatory drugs and past studies have shown the inhibitory effect salicylates have in NF-KB translocation into the nucleus that initiates the inflammation cascade. However, clinically-used high levels of salicylates cause severe adverse side-effects. To overcome this major hurdle, this work proposes the use of biomimetic nanoparticles that selectively deliver salicylates to ICAM-1 expressing retinal endothelial cells. The properties of biocompatibility, biodegradability and non-toxicity along with long circulation times of these NPs and site-targeting capability, we hypothesize that these particles will exhibit superior circulation times, reduced adverse off target effects, and increase drug efficacy by several folds.

Materials and Methods

1. **Synthesis of the RBC nanoparticles**. Bovine blood (Rockland Immunochemicals Inc.) was spun down at 1000 xg for 5 minutes in 1xPBS at pH 7.4. The pellet was separated from the supernatant after each spin and this was done until the supernatant was completely clear. The isolated red blood cell pellet was suspended in 40 mOsm PBS buffer in the ratio of 1:10 (cells: lysis buffer volume) and spun down at 15,000 rpm for 10 minutes at 4 °C (Beckman Coulter Optima XE). This was repeated until a clear white ghost pellet was obtained. The ghost pellet was then resuspended in the drug solution and incubated with the synthetic lipids, 1,2-distearoyl-sn-glycero-3-phosphoethanolamine-N-[Maleimide(polyethylene

glycol)-2000) (DSPE-PEG Maleimide, Avanti Polar Lipids, Inc.) and 1,2-Dihexadecanoyl-sn-Glycero-3-Phosphoethanolamine, Triethylammonium salt (DHPE Texas Red, Invitrogen). All the components were then sonicated with a probe sonicator (Thermo Fisher) for 5 minutes and extruded through 400 nm polycarbonate filter using the Mini-extruder (Avanti Polar Lipids, Inc).

2. **Conjugation and detection of h-scFv on RBC-NL surface.** The extruded RBC-NLs were spun down and h-scFv at a working concentration of 100ug/mL was added to the RBC-NL suspension in 1xPBS at pH 7.1. This is to facilitate the conjugation of h-scFv onto the Maleimide groups. This was incubated overnight at 4 °C. Free cysteine (Sigma Life Sciences, USA) at 20mM working concentration was added to the suspension to quench free Maleimide groups. For the detection and quantification of scFv, mouse anti-his primary antibody that has affinity to the 6-his groups on scFv was added at a working concentration of 0.1175 uM. FITC-conjugated Dy-Light rabbit anti-mouse secondary antibodies (Vector Laboratories, USA) were added in equimolar concentrations for the binding and detection of primary antibodies. Fluorescence measurements were taken using the Flexstation II at 488/540 nm.
3. **Sodium Salicylate incorporation efficiency**. To determine the incorporation of sodium salicylate within the RBC-NL core, the drug incorporated RBC-NLs were rinsed by spinning them down at 4 °C and the supernatant after the rinse was collected. This was added to Ferric Nitrate reagent prepared in 1% Nitric acid to form a blue colored complex. Absorbance measurements at 530 nm of these

samples were taken using the Nanodrop 2000C spectrophotometer (Thermo Scientific). %Drug incorporation (DI) was determined using the formula,

$$\%DI = \frac{Abs\ of\ Total\ drug\ added - Abs\ of\ the\ unincorporated\ drug}{Abs\ of\ Total\ drug\ added} * 100$$

4. **RBC-NL size and morphology characterization**. 200 uL of the RBC-NL loaded with drugs and scFv conjugated RBC-NL were suspended in 1xPBS at pH 7.4. The size distribution was measured using the dynamic light scattering (DLS) using the Delsa Nano C Particle Analyzer (Beckman Coulter, USA). Zeta Potential measurements were also measured using DLS. Microsoft excel and Origin Pro software were used to document and analyze the data. For the SDS-PAGE gel, the RBC ghost and RBC-NLs were spun down to remove any free proteins and the other contaminants. They were lysed using 1x RBC lysis buffer and these lysed samples were subsequently prepared for PAGE gel.
5. **Cell Culture**. Human Retinal Endothelial Cells (HRECs) were purchased from Center for Disease Control (CDC)[36] and cultured on gelatin coated tissue culture dishes in growth media composed of MCDB-131 (VWR International, USA) supplemented with 10% FBS (Fisherbrand, USA), 2 mM L-glutamax, 10ng/mL EGF (Millipore, Sigma), 1 ug/mL hydrocortisone (Sigma Aldrich, USA), 1x antianti, 100 ug/mL heparin sodium salt and 30 ug/mL ECGS. Human U937 monocytic cells were purchased from ATCC (Manassas, VA, USA) and cultured in suspension in growth medium composed of RPMI 1640 (Fisherbrand, USA) supplemented with 2 mM L-Glutamine (Invitrogen), 10 mM HEPES (Fisherbrand, USA), 10% FBS (Fisherbrand), antimycotic/antibiotic mixture (Life Technologies,

USA), 1 mM sodium pyruvate (Life Technologies, USA) and 4.5 mg/ml glucose (Sigma Aldrich, USA).

6. **Uptake of RBC-NLs by HRECs.** To determine the rate of RBC-NL uptake by endothelial cells, Texas Red® labeled RBC-NLs were diluted 1:10 in EC culture media and added to the cells for 0.5, 2, 4 and 8 hrs at 37 °C. The RBC-NLs were rinsed off with 1xPBS Ca^{2+} Mg^{2+} and fixed with 4% PFA. This was then stained with Phalloidin and DAPI, respectively. Cells were mounted and imaged using the Leica Confocal Microscope SP5. To quantify the extent of RBC-NL uptake fluorescence intensity of the perinuclear region and the nuclear region was measured using ImageJ software. The net fluorescence intensity was calculated by subtracting the nuclear fluorescence with perinuclear fluorescence values.
7. **Monocyte-EC adhesion assay**. To evaluate the effects of sodium salicylate, confluent EC monolayers were treated with 10ng/mL of TNF-α (eBiosciences, USA) in HREC starvation media (2.5 %FBS) for 4 hrs prior to the addition of RBC-NLs and scFv conjugated RBC-NLs. The cells were incubated with the NLs for 8 hrs and rinsed with 1xPBS Ca^{2+} Mg^{2+}. The NLs were incubated overnight for the encapsulated drug to be released. The free drug sample was pre-treated with 10mM sodium salicylate and co-treated with 10ng/mL TNF-α and 10mM of the drug for 5 hrs. The RBC-NL treated cells were again TNF-α for 5 hrs. U937 monocytes were added and incubated for 30 minutes at 37 °C. These were rinsed off with 1xPBS Ca^{2+} Mg^{2+} 2-3 times and fixed with 2% PFA for phase contrast imaging. The quantification was done using ImageJ.

8. **Statistics**. All data was obtained from multiple replicates, as stated in the respective figure legends. Data is expressed as the mean ± standard deviation. Statistical significance was determined using ANOVA and followed by Tukey multiple comparison post hoc analysis (Graphpad Inc.).

Results and Discussion

1. Synthesis of RBC membrane derived nanoliposomes (RBC-NLS)

1.1. RBC membrane derived vesicles

Erythrocyte ghosts are obtained after the removal of all intracellular contents of red blood cells. The most common approach used in synthesizing ghosts, is by treating the cells with hypotonic buffer. This primarily removes the intracellular contents and retains the cell membrane. This method produces ghosts with properties similar to or almost identical to the original cell membrane. Hence "hypotonic lysis" has been one of the most widely adopted methods for ghost synthesis [38]. The properties of the final ghost product depend almost entirely on the conditions maintained during the point of lysis and the handling of the resulting ghosts thereafter [38]. By stringently controlling the temperature [39], pH [38], [40], hypotonic buffer strength [41] and the cell: buffer ratio during hemolysis [42], [38], the desired ghost samples can be synthesized. Maximizing the removal of hemoglobin while retaining the membrane's ability to reseal completely has been one of the major goals of this project. Hence, all the conditions for ghost synthesis have been adjusted to produce the desired type of ghosts.

Different strengths of hemolysing buffer and pH combinations were adapted to determine the best condition that would give the desired Type II ghosts, ghosts that reseal completely after hemolysis. As seen in **Fig (1A),** the maximal hemoglobin removal is observed at buffer strengths of 60 mOsm and 40 mOsm. But there is a significant difference between the action of the two buffer strengths **Fig (1B)**. Hence, the best condition of 40 mOsm was chosen as the buffer strength of choice for the removal of hemoglobin. The ghosts were synthesized in a set temperature range of 0-4 °C as literature suggests hemoglobin depletion at higher temperatures leads to the production of leaky ghosts [39], [38]. The pH for lysis was adjusted to 8.0, as studies have shown the most efficient hemoglobin removal occurs at a pH of 8.0 [40]. Also, the pH maintained during hemolysis has an effect on the ghost property even after hemolysis and resealing of the ghosts. This is attributed to the exposure of certain ionizable groups of the lipid membrane or the inability of certain charged entities to be submerged back in the membrane post hemolysis. The conditions during lysis also causes the activation of certain proteolytic or degradative enzymes that might have irreversible effects on the ghosts [38]. Hence, maintaining the pH during the entire process of ghost synthesis is crucial. The cell:hypotonic buffer ratio was maintained to 1:10 as any ratio below this would not be very effective in hemoglobin removal [42].

1.2. Preparation of RBC-NLs

Past studies have shown that particles larger than 200 nm are likely to get phagocytosed by circulating macrophages and cleared by the RES system, while particle smaller than 70 nm get cleared by the kupffer cells of the liver. Commonly used techniques to reduce the size of the multi-lamellar vesicles to nanometer scale include sonication and/or serial extrusion. Though they have different working principles, both these techniques apply mechanical stress on the particles producing large, mostly unilamellar vesicles. To assess which of the two techniques work best in synthesizing RBC-NLs in the desired size range, we measured the size of the particles after probe sonication. But, the Dynamic Light Scattering (DLS) measurements show that probe reduces the size of a fraction of the ghost population but does not bring it down to the desired size range **Fig (2A)**. As sonication did not produce the desired results, extrusion was considered as a method for nanoparticle synthesis. To produce monodisperse population of nanoparticles extrusion though 100 nm filters is necessary [43]. Hence, the RBC ghosts were extruded through 100 nm filters but as the size measurements show this did not produce particles in the required size range **Fig (2B)**. Serial extrusion through 400 nm and 100 nm filters was then performed but surprisingly, no difference in the size was observed **Fig (2C)**. This got us back to using sonication but, this was now followed by extrusion. Both serial extrusion through 400 nm & 100 nm and extrusion only through 400 nm were considered after sonication. As seen from the DLS measurements, extrusion through 400 nm and 400 & 100nm produces the desired size range of nanoparticles of ~100nm **Fig (2D, 2E)**. But this also refutes the need for serial extrusion or extrusion through 100 nm filter which is extremely difficult to accomplish

with RBC ghosts. A critical step that made this process repeatable was rising the temperature of the samples to 37 °C prior to extrusion (data not shown). As this temperature lies within the range of the lipid transition temperature of the phospholipid constituents of the membrane the cyclic passage of RBC ghosts through the nanopores of the membrane is feasible. Also, any temperature above 30 °C has an effect on the structural proteins of RBC ghosts that makes cyclic passage [44].

1.3. Surface modification of RBC-NLs with ICAM-1 targeting scFv

As chronic vascular inflammation is marked by enhanced upregulation of ICAM-1 receptors, nanoparticle surface can be functionalized with specific anti-ICAM-1 IgGs and this can be used for targeting of activated endothelial cells. But the F_c domain of the IgGs activate the complement system and result in active clearance of the antibody-conjugated nanoparticles from circulation. Hence to navigate around this problem, single-chain variable fragment (scFv) that encompasses only the variable region of the antibody can be used as targeting moieties [31]. These engineered scFv fragments consist of free cysteine groups that can interact with other sulfhydryl groups to form disulphide bridges. To aid this interaction, DSPE-PEG Maleimide is incorporated into the RBC-NL lipid membrane. Maleimide forms disulphide bridges with the free cysteine groups of scFv, thus ensuring the adherence of targeting moiety on the nanoparticle surface.

Our lab has used this principle previously with synthetic nanoliposomes and shown successful binding of the scFv fragment onto the nanoliposome surface [31]. But, as the RBC membrane is more complex compared to synthetic nanoliposomes due to the presence

of glycolipids and glycoproteins, we wanted to verify if incorporation of PEG-Maleimide into RBC ghost membrane is necessary for surface functionalization with scFv. The comparison was done by incorporating 1,2-diphytanoyl-sn-glycero-3-phosphocholine (Dphpc), a saturated lipid with no known thiol groups and 1,2-distearoyl-sn-glycero-3-phosphoethanolamine-N-[Maleimide(polyethylene glycol)-2000) (DSPE-PEG Maleimide). Quantitative fluorescence analysis **Fig (3A)**, shows an approximately ~5-fold increase in the binding of scFv antibody fragments to PEG-Maleimide incorporated surface compared to membrane with no known thiol group. This substantiates the need to incorporate synthetic DSPE-PEG-Maleimide into the RBC lipid membrane as it improves the binding of scFv onto the NL surface.

The effect of mechanical extrusion and sonication on scFv conjugation was verified and as shown in **Fig (3B, 3C)**, subjecting the ghosts through the aforementioned mechanical stresses does not affect scFv binding. Further, DLS measurements reveal that conjugating scFv on the surface exhibits a narrow size range of 118.4 ± 23.0 nm which is the preferred size range (70-200 nm) for long circulating nanoparticles.

2. Loading Sodium Salicylate into RBC-NLs

As mentioned previously, high concentrations of sodium salicylates have adverse side effects on various parts of the body. But, high doses of salicylates are required for noticeable anti-inflammatory effects on DR. Adopting nanotherapeutics might ameliorate most of these adverse side effects. As sodium salicylate is hydrophilic in nature the drug gets encapsulated within the core of the RBC-NLs and remains protected by the lipid

bilayer. Various methods have been proposed for drug loading into the nanoparticle core but the strategy used depends almost entirely on the properties of the drug being encapsulated [45]. Based on this, we decided to adopt the osmotic method of hypotonic hemolysis, where the drug is loaded through the pores that are created during lysis. This is followed by the resealing step with a hypertonic buffer that essentially closes the pores on the membrane surface to retain the loaded drugs.

To determine the point of introduction of the drug after lysis two approaches were considered, for proof of principle studies fluorescein was chosen as the solute to be incorporated as this is easier to detect. In the first approach, fluorescein was loaded into the ghosts right after hemolysis when the membrane pores are still open. The dye loaded ghosts were then resealed at two different temperatures of 37 °C for 1 hour vs 4 °C overnight. These were subsequently sonicated and extruded to synthesize RBC-NLs. Quantitative fluorescence measurements show low incorporation efficiencies using this method of dye loading. Also, the data suggests a possible role of resealing temperature in incorporation efficiency as lower incorporation is seen with samples resealed at 37 °C.

In the second approach, the dye was introduced right after hemolysis but unlike the previous approach these particles were sonicated and extruded while suspended in the dye solution and then resealed at 37 °C for 1 hour vs 4 °C overnight. This approach gave higher incorporation efficiency and the values being higher when the RBC-NLs were resealed at 4 °C **Fig (4A)**. The same method was used for drug loading into the RBC-NLs and the maximum drug incorporation was observed to be at 31 mM of sodium salicylate loading with ~ 45 % incorporation efficiency. DLS measurements further confirmed that drug

loading and modification with scFv maintained the particles size in the narrow size range. **Fig (4B**).

3. Characterization of RBC-NLs

3.1. PAGE-gel of RBC ghosts and RBC-NLs surface membrane proteins

Protein retention by the RBC-NLs after sonication and mechanical extrusion was examined by running a protein gel of the RBC-NLs along with RBC ghosts. The protein gel indicates that most of the membrane proteins are retained by the RBC-NLs. As the bands corresponding to the major and minor protein bands are still comparable. The major integral membrane protein band 3 and structural protein band 4.1R, which maintains the structural integrity and stability of the membrane is still retained by the RBC-NLs. A noticeable loss is seen with spectrin that is associated with cell cytoskeleton. The bands corresponding to both the α and β chains of spectrin are fainter with the RBC-NL sample in comparison to RBC-ghosts. But, this could be explained by the fact that ghosts are reduced in size as a result the bigger proteins cannot be accommodated in the membrane anymore and hence the loss.

3.2. Determination of RBC-NL stability and shelf-life

Size and Aggregation

The stability of RBC-NLs stored at 4 °C was evaluated over 2 weeks. The size of the RBC-NLs was measured using dynamic light scattering (DLS). The sizes of the unconjugated RBC-NL sample and the scFv conjugated RBC-NL sample are

comparable when synthesized. But, based on the Polydispersity Index values (PDI) the scFv conjugated RBC-NL samples are comparatively more monodisperse than the RBC-NL samples. This implies that the scFv conjugated RBC-NLs is a more uniform suspension compared to the RBC-NL samples. With storage, a portion of the RBC-NL samples and the scFv conjugated samples start clumping together to form aggregates **Fig (6A), (6B)**. This can be seen within 4 days of storage. But, in comparison with scFv conjugated RBC-NLs the unconjugated RBC-NLs start forming bigger aggregates with time.

Zeta potential values

The zeta potential values give a measure of the surface charge distribution of the nanoparticles in a colloidal suspension. The higher the absolute value of the parameter, the higher is the repulsive forces between the nanoparticles as a result, lower chances of them forming aggregates. This means that the colloidal suspension is more stable. The zeta potential values of our RBC-NL samples is comparable with values cited in the literature for erythrocyte membrane based particles [46] which is ~ -15 mV. Also, zeta potential values of the scFv conjugated samples are similar to that of RBC-NLs suggesting that the surface modification with antibody fragment does not affect the charge distribution of the particles **Fig (6A)**.

4. Cellular uptake of RBC-NLs

4.1. Uptake of RBC-NLs by cultured HRECs

After synthesis and characterization of the nanoliposomes, we examined the uptake of RBC-NLs by cultured HRECs. DHPE-Texas Red incorporated RBC-NLs were added to the endothelial cells for 0.5, 2, 4 and 8 hours prior to fixation and imaging. Quantification of the images revealed that 0.5 – 2 hours of incubation is insufficient for HRECs to uptake nanoparticles as there is no significant difference between these conditions and the control, as in **Fig 7**. However, a significant increase in uptake is observed with 4-hour incubation, with the trend increasing further with at the 8 hr \time point, as shown in **Fig 7**. Consistent with past studies form our and other groups [47], [36], [48], the fluorescently labelled RBC-NLs localized within the perinuclear region, suggesting the endocytic mode of uptake by the acidic organelles viz. lysosomes and endosomes lining the perinuclear region.

4.2. Uptake of scFv conjugated RBC-NLs by HRECs

Endothelial ICAM-1 expression was upregulated by treating HRECs with Tumor Necrosis Factor-α (TNF-α), which is a pro-inflammatory factor that is upregulated in inflammatory conditions and causes increased expression of ICAM-1. scFv conjugated RBC-NLs and RBC-NLs were added to TNF-α treated and untreated HREC cultures for 8 hrs. Confocal imaging and subsequent fluorescence analysis using ImageJ reveals ~2-fold preferential uptake of scFv conjugated RBC-NLs compared to RBC-NLs, as

shown in **Fig 8**. This serves as the proof of principle for the preferential targeting of scFv to ICAM-1 expressing ECs.

5. Anti-inflammatory effects of Sodium Salicylate

5.1. Sodium Salicylate exerts Anti-Inflammatory effects on Activated HRECs

Sodium Salicylate is a known anti-inflammatory drug that inhibits the NF- KB translocation into the nucleus and then prevents the expression of inflammatory receptors on the endothelial cell surface [16]. We wanted to check if sodium salicylate exhibits the same trend in HRECs. To address this question, HREC monolayers were pre-treated with different doses of sodium salicylate and co-treated with the drug and TNF-α (10ng/mL), a known inflammatory cytokine, to enhance monocyte-EC adhesion both *in-vitro* and in its pathological conditions *in-vivo*. Phase contrast images of adherent U937 cells and its quantification revealed that the addition of sodium salicylate to TNF-α treated cells produces a dose-dependent inhibition of U937 cell adhesion to HRECs (**Fig 9**), with the inhibition being highest at 10 mM dose of the drug, which is comparable to the levels seen in untreated HRECs.

5.2. Encapsulated sodium salicylate has higher drug efficacy than free drug

To ascertain the therapeutic potential of encapsulated drug endothelial cells we performed the U937 cell adhesion assay. HRECs were treated with TNF-α to increase the expression of ICAM-1 that binds U937 monocytes. Sodium salicylate loaded RBC-NLs (31mM, 45% incorporation) were incubated with TNF-α treated cells overnight

and then U937 cells were added to measure of anti-inflammatory potential of encapsulated drug by its virtue of inhibiting the adhesion of U937 cells. To estimate the therapeutic efficacy of the drug, the fluorescence values of the supernatant after 8 hr incubation and uptake was measured along with the fluorescence of the total nanoparticles in cell culture medium that were initially added to the cells. As shown in **Fig 10**, encapsulated drug has comparable effects as the free drug. Also, based on the fluorescence measurements and calculations, encapsulated drug shows an ~700-fold greater drug efficacy than the free drug.

Conclusions

As a proof-of-principle, this study shows the successful development of RBC membrane derived nanoliposomes with a size that falls in the desired size range of 70-200nm for circulating nanoparticles. The characterization of surface proteins via SDS-PAGE gel reveals the retention of majority of the proteins by the RBC-NLs. The stability profiles show that the samples start forming aggregates within 4 days of storage at 4 °C. Also, the surface modification of the RBC-NLs with scFv does not affect the zeta potential as much. This is important because zeta potential determines the stability of the nanoparticle suspension. *In vitro* studies show the surface modification of RBC-NLs with scFv antibody fragments confer a ~2-fold greater selective binding potential to activated HRECs. While the monocyte-EC adhesion assay shows a ~700-fold greater drug efficacy of encapsulated drug compared to free drug.

Figures

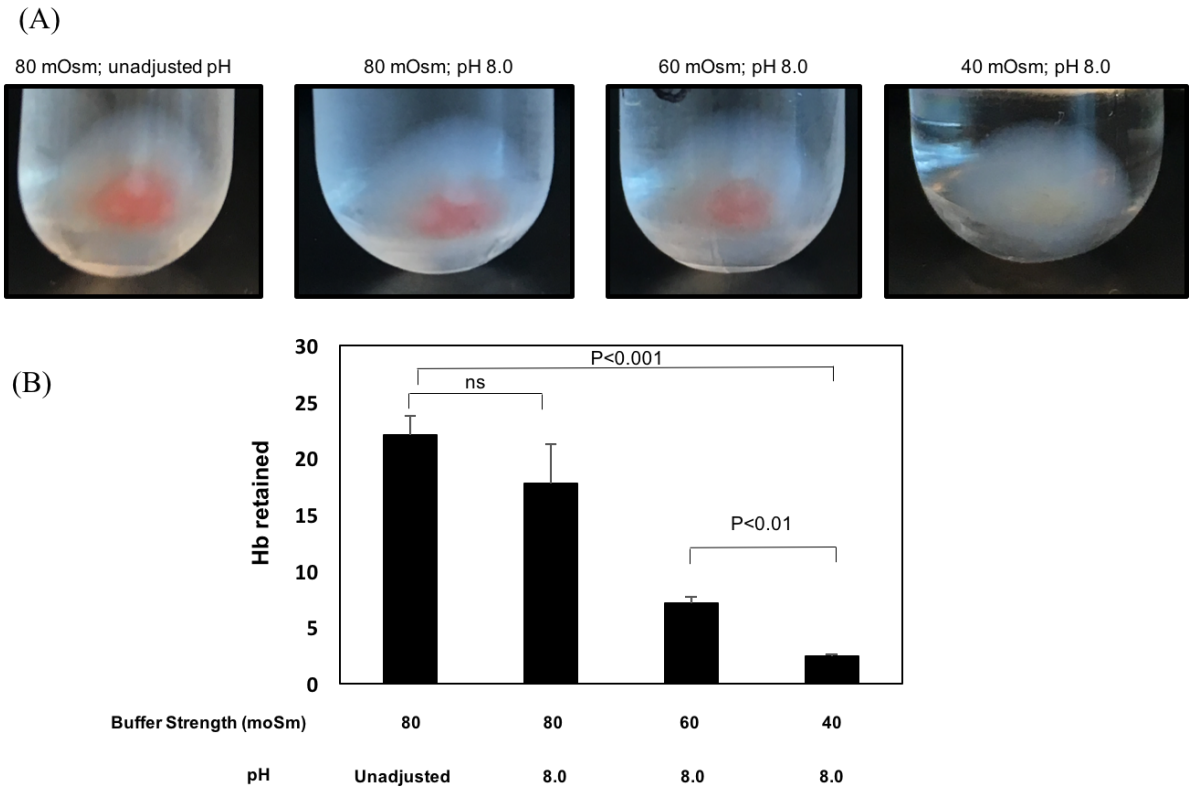

Figure 1: The ghosts were synthesized after the depletion of hemoglobin by subjecting the isolated red blood cells to hemolysis with PBS of different buffer strengths and conditions as described above. The amount of hemoglobin retained by the ghosts were quantified by measuring the Integrated Density of the pellet using ImageJ (Y-axis). Data plotted is the Mean ± SD, n=3.

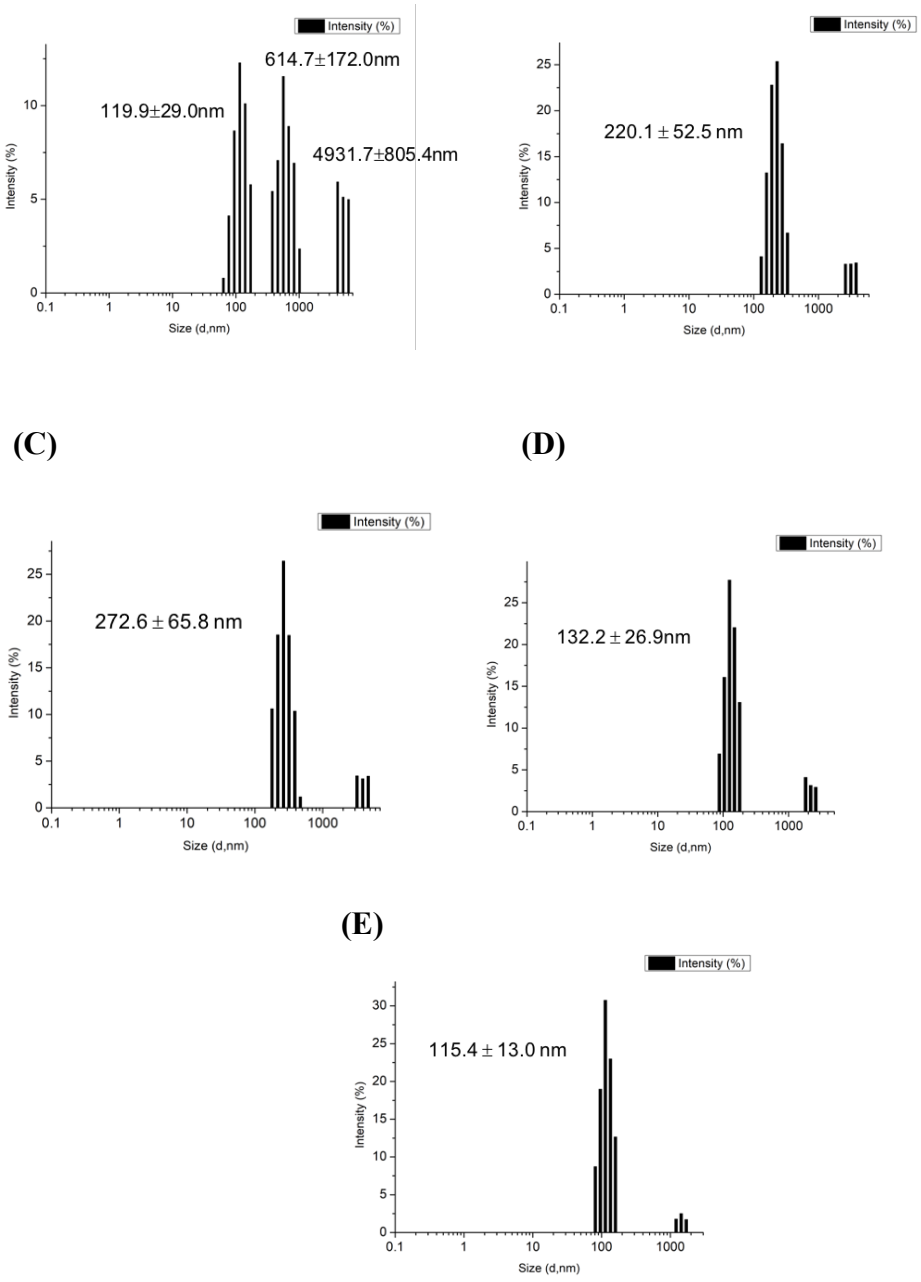

Figure 2: DLS measurements of the RBC nanoparticles subjected to various forms of resizing techniques (A) The RBC ghost samples were sonicated using a probe sonicator for 5 minutes (40 kHz, Thermo Fisher) (B) Extrusion through 100nm (C) Extrusion through 400 & 100 nm (D) Sonication & serial extrusion through 400 followed by 100 nm (E) Sonication and extrusion through 400 nm. PDI of all of them PDI<0.1.

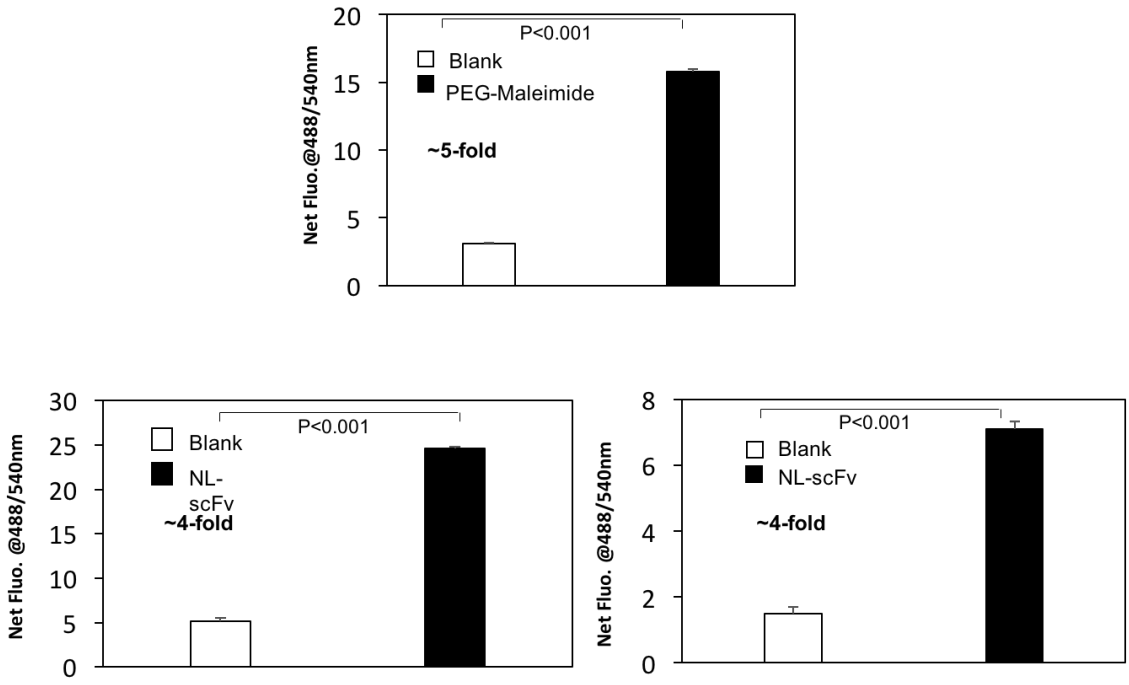

Figure 3: Conjugation of h-scFv onto the surface of RBC-NLs was accomplished by utilizing the spontaneous disulphide bonds that are formed between the free cysteine groups on the scFv and the DSPE-PEG Maleimide that is infused within the RBC membrane. For detection and quantification, anti-his antibodies with specificity to the 6 his groups on h-scFv was added primary antibody(A) Dphpc and PEG-Maleimide was incorporated into the membrane in equal concentrations to determine the advantage Maleimide group would provide. (B) synthesized only with extrusion (C) synthesized with extrusion and sonication. Data plotted is Mean ± SD, n=5.

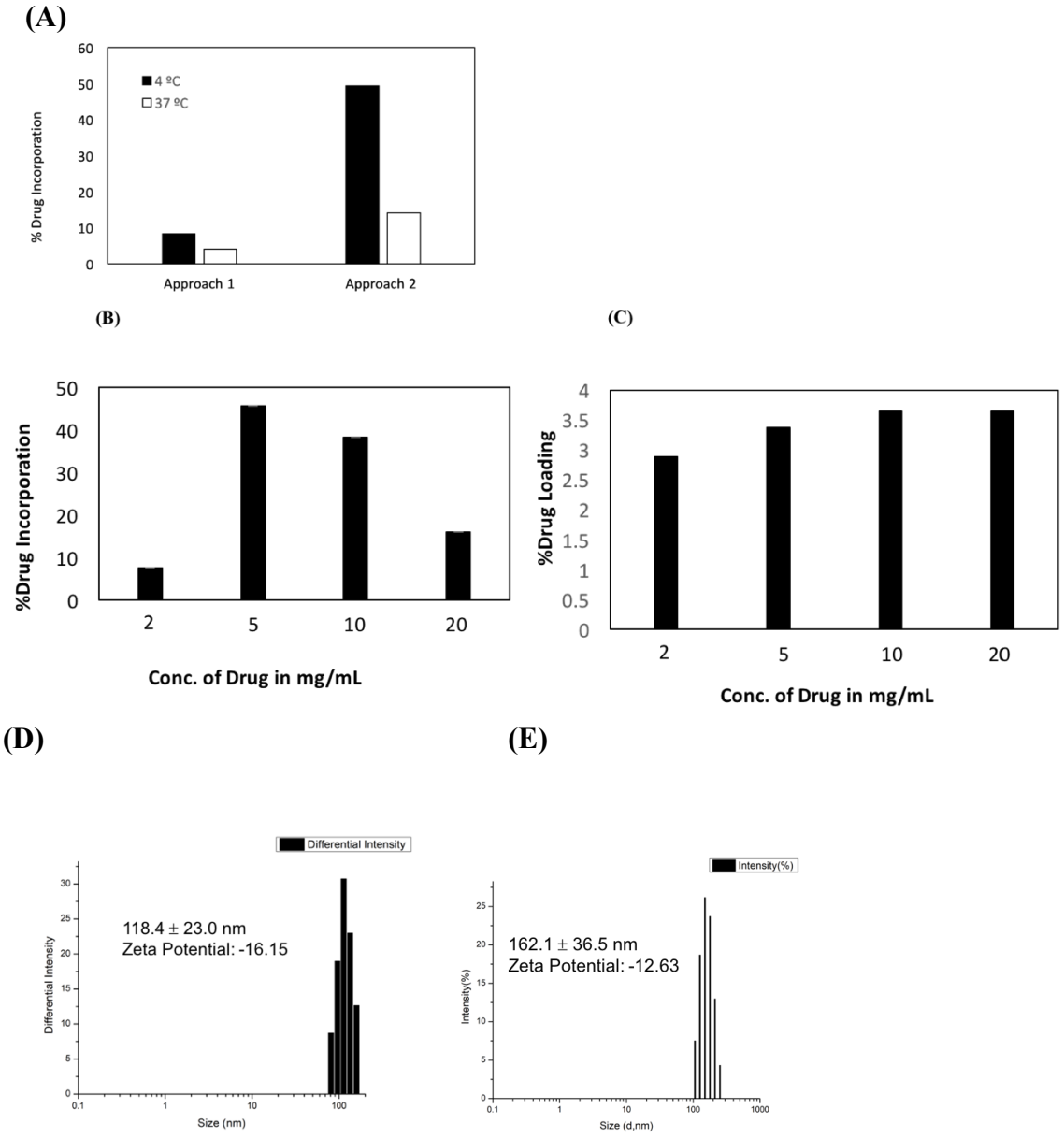

Figure 4: (A) Drug incorporation efficiency was estimated for the two approaches tried for the drug introduction and resealing temperatures. 1 mM of sodium fluorescein was packed into the RBC core. **(B)** The dose dependent incorporation of efficiency of sodium salicylate that was loaded into the RBC-NLs via approach 2. Maximum incorporation efficiency is 45% at 5mg/mL concentration of drug. **(C)** Represents the amount of loaded drug into the RBC-NLs. The core of the NL saturates at a concentration of 10mg/mL of sodium salicylate. Data plotted is % incorporation and loading calculated as described.
(D) Shows the DLS measurements of the Drug loaded NL **(E)** Shows the DLS measurements of the particle loaded with drug and modified with scFv.

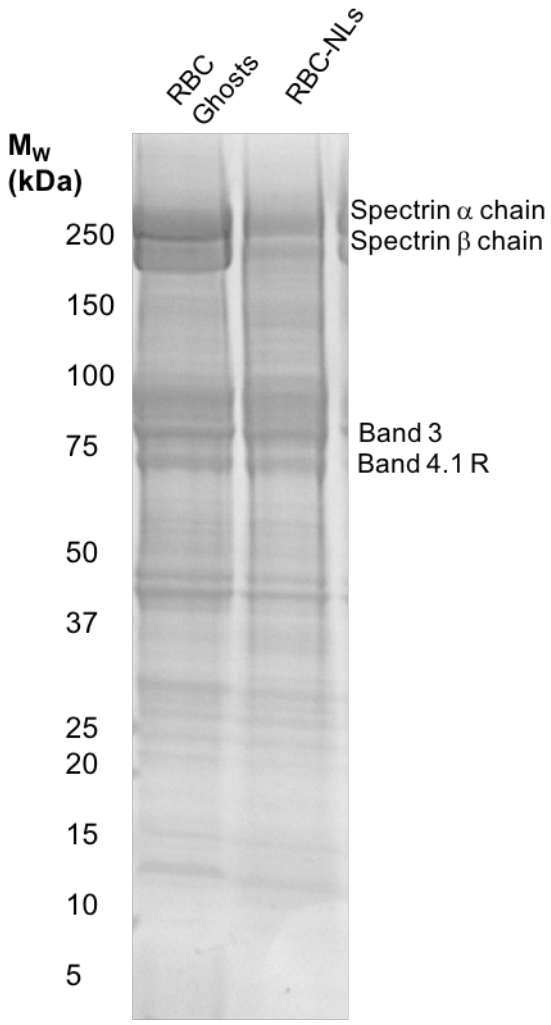

Figure 5: SDS-PAGE of RBC ghosts synthesized by hypotonic lysis and which were later sonicated and extruded to produce RBC-NLs. The samples were lysed with 1x RBC lysis buffer. Spun down to remove the free-floating proteins and samples were prepared for SDS gel.

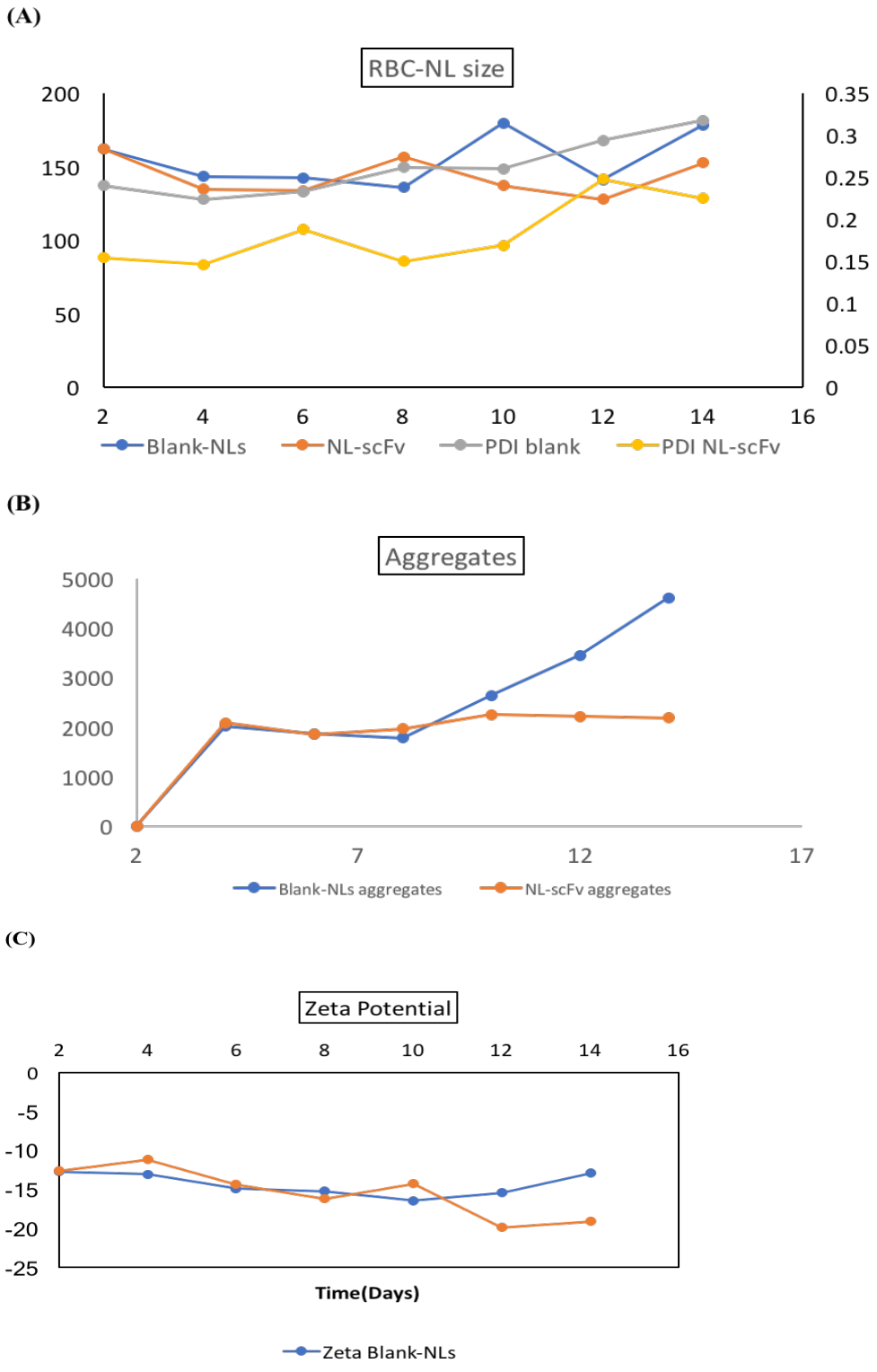

Figure 6: The DLS measurements of the size, PDI, zeta potential of RBC-NL over 16 days.

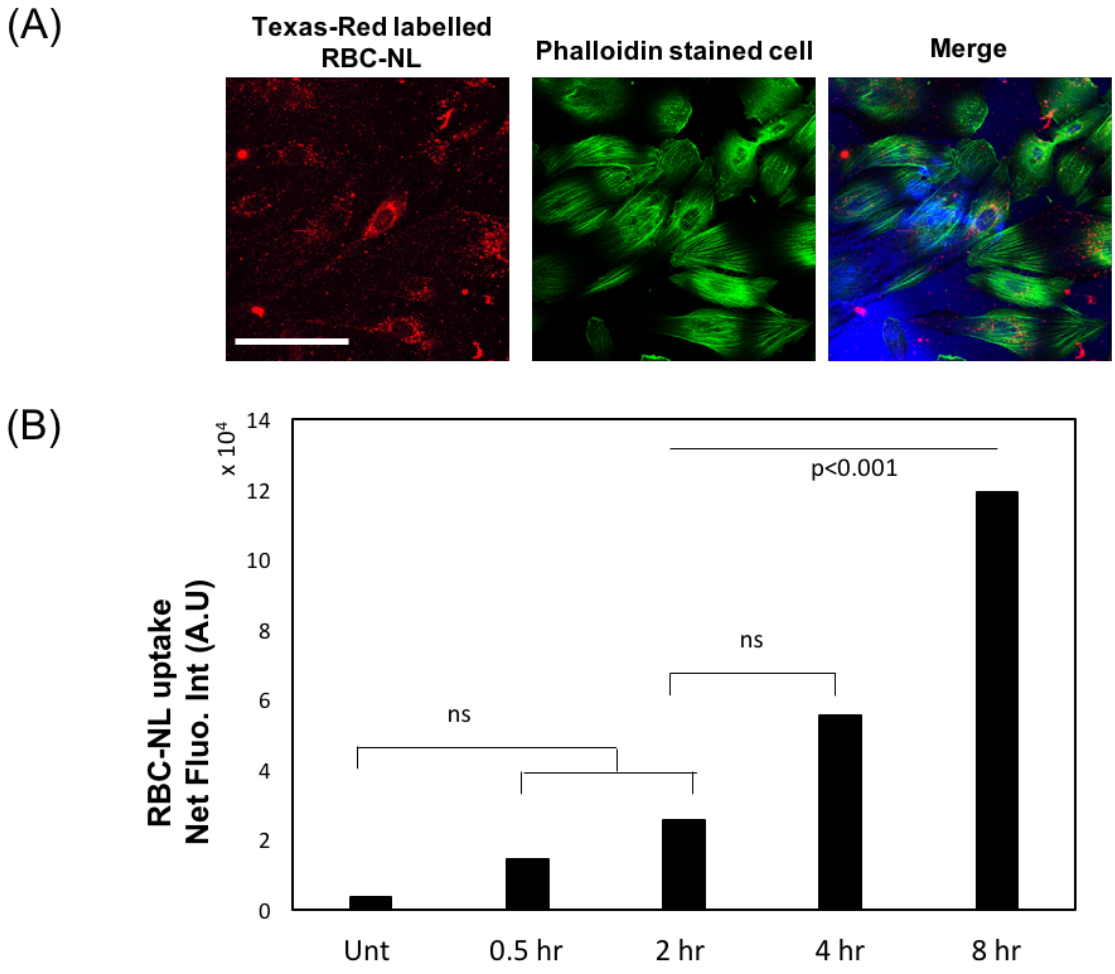

Figure 7: **(A)** DHPE-Texas Red incorporated RBC-NLs were incubated with cultured endothelial cells for different time points. Confocal Imaging reveals the co-localization of RBC-NLs within the perinuclear region, Scale bar= 100 um **(B)** Quantification of the fluorescence intensity of the perinuclear area using ImageJ reveals significant increase in the uptake of NLs by endothelial cells even at 8 hrs. (n=5 images). Data are expressed as Mean ± SD.

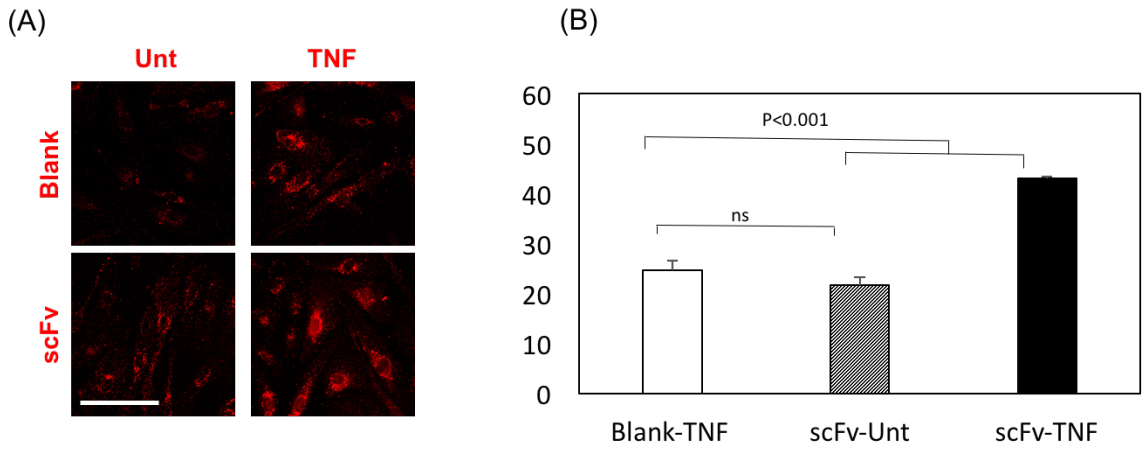

Figure 8: (A) DHPE-Texas Red incorporated scFv conjugated RBC-NLs and unconjugated RBC-NLs were incubated with cultured endothelial cells for 8 hours. Confocal Imaging reveals the co-localization of RBC-NLs within the perinuclear region, Scale bar= 100 um. **(B)** Quantification of the fluorescence intensity of the perinuclear area using ImageJ reveals ~2-fold greater uptake of scFv conjugated RBC-NLs compared to unconjugated RBC-NLs by TNF-α activated retinal endothelial cells. (n=3 images with n=5 cells per FOV). Data are expressed as Mean ± SD.

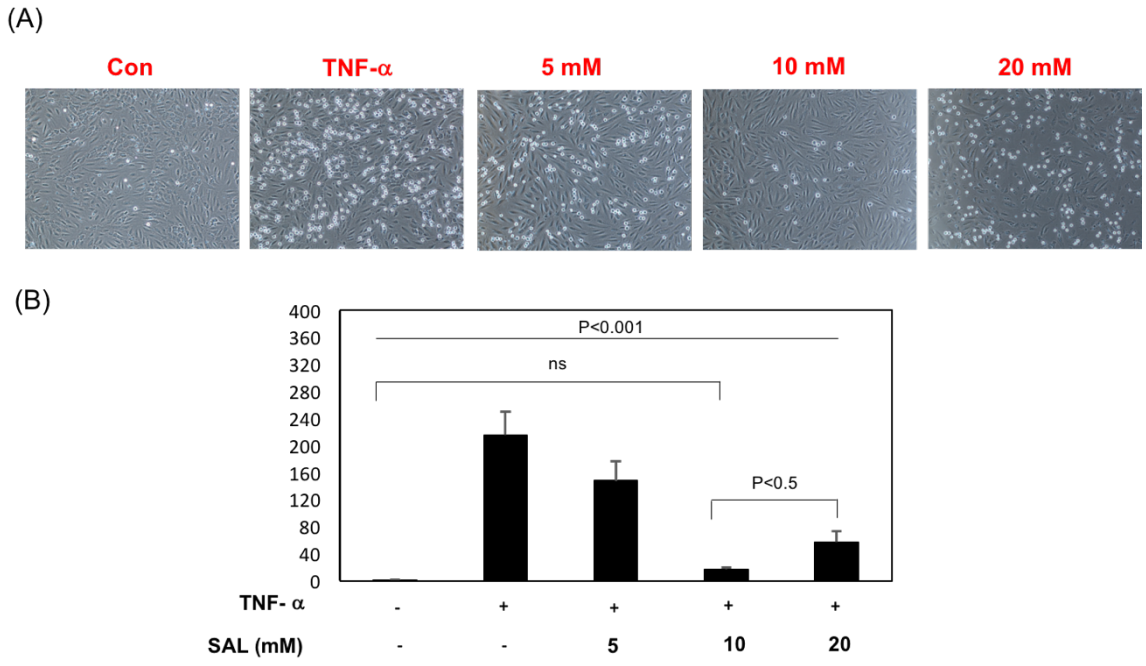

Figure 9: **(A)** Phase contrast images of the endothelial culture with bound U937 cells. Scale bar=100 um. **(B)** Quantification of the U937 cells using ImageJ show dose dependent effect of free sodium salicylate on endothelial cells with potent response at 10 mM dose of the drug. Data are expressed as Mean ± SEM

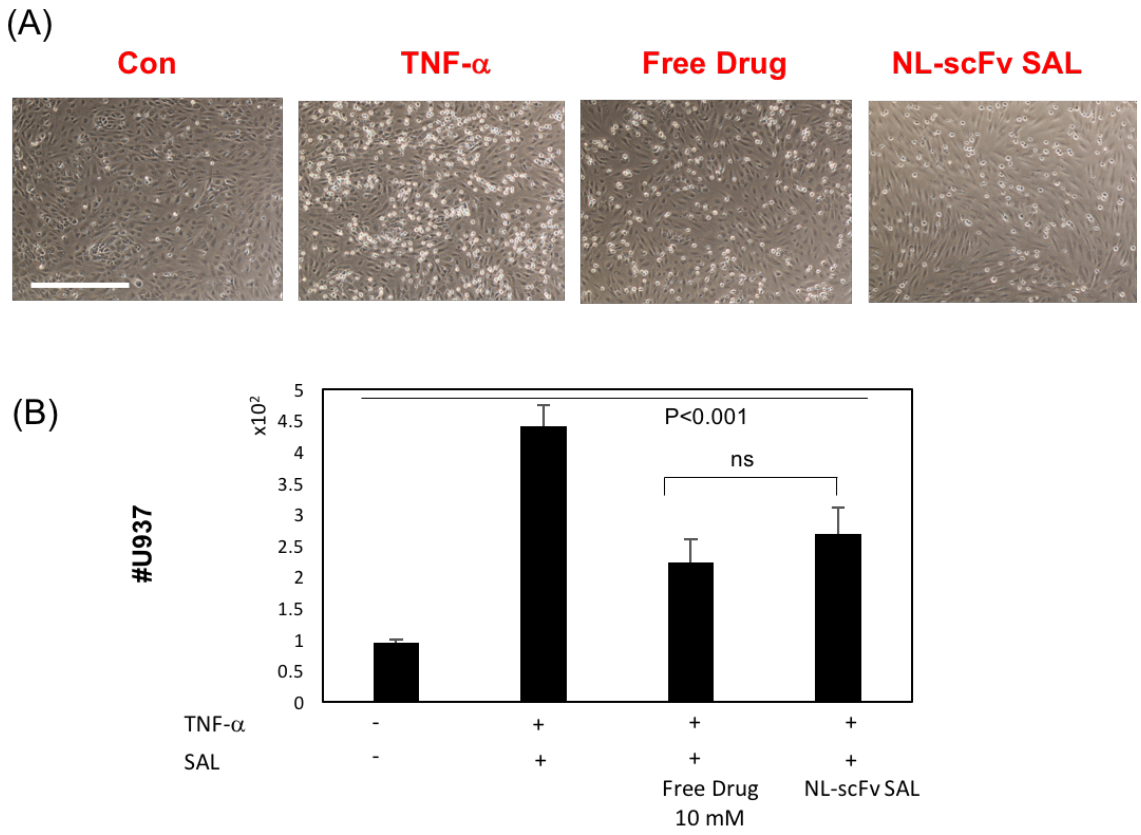

Figure 10: **(A)** Phase contrast images of the endothelial culture with bound U937 cells. Scale bar=100 um. **(B)** Quantification of the U937 cells using ImageJ show no significant difference between Free Drug and NL-SAL but measurements suggest ~700-fold greater drug efficacy of encapsulated SAL. Data are expressed as Mean ± SD.

CHAPTER-3

Conclusion and Future Directions

Using a combination of qualitative and quantitative methods, it was demonstrated that biomimetic nanoparticles, specifically red blood cell membrane derived nanoparticles, can be designed for site-targeted drug delivery. Detailed physicochemical characterization exhibited that these nanoparticles lie in the desired size range, they successfully undergo surface modification by conjugating anti-ICAM-1 h-scFv and encapsulate drug within the NL core. *In vitro* studies further corroborate the site-targeting capability of surface modified RBC-NLs with the preferential uptake of scFv conjugated nanoliposomes by activated retinal endothelial cells and the inflammation assay shows the superior drug efficacy of encapsulated drugs. This enhances the benefit/risk profile of sodium salicylate therapy for inflammation mediated vascular complications of the eye. This serves as a proof-of-principle for the use of cell membrane derived/biomimetic particles for targeted drug delivery.

Though liposomal synthetic nanoparticles have the advantage of rationale design and better material control, rapid clearance from the body has always been a major concern. This has also been a major hurdle in translating this technology to clinical use. The endogenous properties of biomimetic particles can potentially overcome this major drawback. But, this conclusion would be purely theoretical unless a direct comparison is made between the

liposomal synthetic nanoparticles and RBC-NLs. As a result, *in-vivo* studies in mouse models looking at the circulation times of both these particles injected in equal concentrations would provide evidence for the believed superior immune masking properties of the red blood cell membrane derived NLs.

As the major focus of this project was to establish a proof-of-principle for the use of cell derived particles for drug delivery, RBC-NLs are currently derived from Bovine blood but to perform mice studies the transition to NLs derived from mouse blood is necessary. The method of synthesis would be the same except for few optimizations, if necessary. Also, the exact concentration of these particles in a suspension needs to be estimated to make accurate deductions from the *in-vivo* studies.

In vitro studies suggest a preferential binding and uptake of scFv conjugated RBC-NLs. This would potentially improve the biodistribution profile of the NLs as these particles would home selectively to inflamed endothelial cells. This needs to be confirmed in diabetic mice models with inflamed retina and the percent retention of these particles in the blood and the percent clearance by the RES system needs to be studied at different time points.

The inflammation assay involving the quantification of adherent U937 cells shows a higher drug efficacy of the encapsulated drugs. But, it needs to be checked if this observation is consistent *in vivo*. Drug loss during circulation, drug efficacy of encapsulated drug, and its

ability to successfully reduce the leukocyte adhesion to retinal ECs need to be estimated in a diabetic vascular inflammation model.

Past studies have shown the long-term effects of salicylates on vascular inflammation [18], [17], [16]. But inhibiting DR pathogenesis through the use of RBC-NLs with encapsulated anti-inflammatory drugs over the long term needs to be studied. The potential of encapsulated drug in successfully inhibiting the pathogenesis and further progression also needs to be evaluated.

References:

[1] N. H. Cho *et al.*, "IDF Diabetes Atlas: Global estimates of diabetes prevalence for 2017 and projections for 2045," *Diabetes Res. Clin. Pract.*, vol. 138, pp. 271–281, 2018.

[2] Y. Zheng, M. He, and N. Congdon, "The worldwide epidemic of diabetic retinopathy," *Indian J. Ophthalmol.*, vol. 60, no. 5, p. 428, 2012.

[3] E. J. Duh, J. K. Sun, and A. W. Stitt, "Diabetic retinopathy: current understanding, mechanisms, and treatment strategies," *JCI Insight*, vol. 2, no. 14, 2017.

[4] K. Shimizu, Y. Kobayashi, and K. Muraoka, "Midperipheral fundus involvement in diabetic retinopathy," *Ophthalmology*, vol. 88, no. 7, pp. 601–612, 1981.

[5] G. L. King, A. B. Berman, S. Bonner-Weir, and M. P. Carson, "Regulation of vascular permeability in cell culture," *Diabetes*, vol. 36, no. 12, pp. 1460–1467, 1987.

[6] D. R. S. R. Group, "Preliminary report on effects of photocoagulation therapy," *Am. J. Ophthalmol.*, vol. 81, no. 4, pp. 383–396, 1976.

[7] P. A. Campochiaro *et al.*, "Sustained delivery fluocinolone acetonide vitreous inserts provide benefit for at least 3 years in patients with diabetic macular edema," *Ophthalmology*, vol. 119, no. 10, pp. 2125–2132, 2012.

[8] D. S. Boyer *et al.*, "Three-year, randomized, sham-controlled trial of dexamethasone intravitreal implant in patients with diabetic macular edema," *Ophthalmology*, vol. 121, no. 10, pp. 1904–1914, 2014.

[9] R. L. Avery *et al.*, "Intravitreal bevacizumab (Avastin) in the treatment of proliferative diabetic retinopathy," *Ophthalmology*, vol. 113, no. 10, pp. 1695–1705, 2006.

[10] A. M. Joussen *et al.*, "A central role for inflammation in the pathogenesis of diabetic retinopathy," *FASEB J.*, vol. 18, no. 12, pp. 1450–1452, 2004.

[11] K. Miyamoto *et al.*, "Prevention of leukostasis and vascular leakage in streptozotocin-induced diabetic retinopathy via intercellular adhesion molecule-1 inhibition," *Proc. Natl. Acad. Sci.*, vol. 96, no. 19, pp. 10836–10841, 1999.

[12] J. Tang *et al.*, "MyD88-dependent pathways in leukocytes affect the retina in diabetes," *PloS One*, vol. 8, no. 7, p. e68871, 2013.

[13] A. P. Adamis, *Is diabetic retinopathy an inflammatory disease?* BMJ Publishing Group Ltd, 2002.

[14] N. Nagai *et al.*, "Suppression of diabetes-induced retinal inflammation by blocking the angiotensin II type 1 receptor or its downstream nuclear factor-κB pathway," *Invest. Ophthalmol. Vis. Sci.*, vol. 48, no. 9, pp. 4342–4350, 2007.

[15] E. Iliaki, V. Poulaki, N. Mitsiades, C. S. Mitsiades, J. W. Miller, and E. S. Gragoudas, "Role of α4 integrin (CD49d) in the pathogenesis of diabetic retinopathy," *Invest. Ophthalmol. Vis. Sci.*, vol. 50, no. 10, pp. 4898–4904, 2009.

[16] L. Zheng, S. J. Howell, D. A. Hatala, K. Huang, and T. S. Kern, "Salicylate-based anti-inflammatory drugs inhibit the early lesion of diabetic retinopathy," *Diabetes*, vol. 56, no. 2, pp. 337–345, 2007.

[17] T. S. Kern and R. L. Engerman, "Pharmacological inhibition of diabetic retinopathy: aminoguanidine and aspirin," *Diabetes*, vol. 50, no. 7, pp. 1636–1642, 2001.

[18] J. Tang and T. S. Kern, "Inflammation in diabetic retinopathy," *Prog. Retin. Eye Res.*, vol. 30, no. 5, pp. 343–358, 2011.

[19] A. M. Joussen *et al.*, "Nonsteroidal anti-inflammatory drugs prevent early diabetic retinopathy via TNF-α suppression," *FASEB J.*, vol. 16, no. 3, pp. 438–440, 2002.

[20] A. Hafner, J. Lovrić, G. P. Lakoš, and I. Pepić, "Nanotherapeutics in the EU: an overview on current state and future directions," *Int. J. Nanomedicine*, vol. 9, pp. 1005–1023, Feb. 2014.

[21] T. Lammers, F. Kiessling, W. E. Hennink, and G. Storm, "Drug targeting to tumors: principles, pitfalls and (pre-) clinical progress," *J. Controlled Release*, vol. 161, no. 2, pp. 175–187, 2012.

[22] T. M. Fahmy, P. M. Fong, A. Goyal, and W. M. Saltzman, "Targeted for drug delivery," *Mater. Today*, vol. 8, no. 8, Supplement, pp. 18–26, Aug. 2005.

[23] Carlos H.Villa, A. C. Anselmo, S. Mitragotri, and V. Muzykantov, "Red blood cells: Supercarriers for drugs, biologicals, and nanoparticles and inspiration for advanced delivery systems," *Adv. Drug Deliv. Rev.*, Feb. 2016.

[24] S. M. Moghimi, A. C. Hunter, and J. C. Murray, "Long-circulating and target-specific nanoparticles: theory to practice," *Pharmacol. Rev.*, vol. 53, no. 2, pp. 283–318, 2001.

[25] T. Ishida, X. Wang, T. Shimizu, K. Nawata, and H. Kiwada, “PEGylated liposomes elicit an anti-PEG IgM response in a T cell-independent manner,” *J. Controlled Release*, vol. 122, no. 3, pp. 349–355, 2007.

[26] X. Wang, T. Ishida, and H. Kiwada, “Anti-PEG IgM elicited by injection of liposomes is involved in the enhanced blood clearance of a subsequent dose of PEGylated liposomes,” *J. Controlled Release*, vol. 119, no. 2, pp. 236–244, 2007.

[27] Chan JM, Valencia PM, Zhang L, Langer R, Farokhzad OC. Polymeric nanoparticles for, “Polymeric nanoparticles for drug delivery.,” *Methods Mol Biol 2010*, vol. 624, pp. 163–175.

[28] C. Gutiérrez Millán, C. I. Colino Gandarillas, M. L. Sayalero Marinero, and J. M. Lanao, “Cell-based drug-delivery platforms,” *Ther. Deliv.*, vol. 3, no. 1, pp. 25–41, 2012.

[29] K. Jin, Z. Luo, B. Zhang, and Z. Pang, “Biomimetic nanoparticles for inflammation targeting,” *Acta Pharm. Sin. B*, 2017.

[30] A. Feinstein, N. Richardson, and M. I. Taussig, “Immunoglobulin flexibility in complement activation,” *Immunol. Today*, vol. 7, no. 6, pp. 169–174, 1986.

[31] S. Ardekani, S. Eum, D. H. Nam, X. Ge, and K. Ghosh, “Anti-ICAM-1 scFv-modified Nanoliposomes for Site-targeted Anti-inflammatory Therapy.”

[32] V. R. Muzykantov, “Drug delivery by red blood cells: vascular carriers designed by mother nature,” *Expert Opin. Drug Deliv.*, vol. 7, no. 4, pp. 403–427, 2010.

[33] J.-W. Yoo, D. J. Irvine, D. E. Discher, and S. Mitragotri, “Bio-inspired, bioengineered and biomimetic drug delivery carriers,” *Nat. Rev. Drug Discov.*, vol. 10, no. 7, p. 521, 2011.

[34] J. T. Mac, V. Nuñez, J. M. Burns, Y. A. Guerrero, V. I. Vullev, and B. Anvari, “Erythrocyte-derived nano-probes functionalized with antibodies for targeted near infrared fluorescence imaging of cancer cells,” *Biomed. Opt. Express*, vol. 7, no. 4, pp. 1311–1322, 2016.

[35] R. K. Tsai, P. L. Rodriguez, and D. E. Discher, “Self inhibition of phagocytosis: the affinity of ‘marker of self’CD47 for SIRPα dictates potency of inhibition but only at low expression levels,” *Blood Cells. Mol. Dis.*, vol. 45, no. 1, pp. 67–74, 2010.

[36] K. Ghosh, M. Kanapathipillai, N. Korin, J. R. McCarthy, and D. E. Ingber, "Polymeric nanomaterials for islet targeting and immunotherapeutic delivery," *Nano Lett.*, vol. 12, no. 1, pp. 203–208, 2011.

[37] P. Kolhar *et al.*, "Using shape effects to target antibody-coated nanoparticles to lung and brain endothelium," *Proc. Natl. Acad. Sci.*, vol. 110, no. 26, pp. 10753–10758, 2013.

[38] G. Schwoch and H. Passow, "Preparation and properties of human erythrocyte ghosts," *Mol. Cell. Biochem.*, vol. 2, no. 2, pp. 197–218, 1973.

[39] H. Bodemann and H. Passow, "Factors controlling the resealing of the membrane of human erythrocyte ghosts after hypotonic hemolysis," *J. Membr. Biol.*, vol. 8, no. 1, pp. 1–26, 1972.

[40] J. T. Dodge, C. Mitchell, and D. J. Hanahan, "The preparation and chemical characteristics of Hemoglobin-free ghosts of human erythrocytes."

[41] T. A. Bramley, R. Coleman, and J. B. Finean, "Chemical, enzymological and permeability properties of human erythrocyte ghosts prepared by hypotonic lysis in media of different osmolarities," *Biochim. Biophys. Acta BBA-Biomembr.*, vol. 241, no. 3, pp. 752–769, 1971.

[42] T. Teorell, "Permeability properties of erythrocyte ghosts," *J. Gen. Physiol.*, vol. 35, no. 5, pp. 669–701, 1952.

[43] T. F. Zhu and J. W. Szostak, "Preparation of large monodisperse vesicles," *PloS One*, vol. 4, no. 4, p. e5009, 2009.

[44] G. M. Artmann, C. Kelemen, D. Porst, G. Büldt, and S. Chien, "Temperature transitions of protein properties in human red blood cells," *Biophys. J.*, vol. 75, no. 6, pp. 3179–3183, 1998.

[45] C. G. Millan, M. L. S. Marinero, A. Z. Castaneda, and J. M. Lanao, "Drug, enzyme and peptide delivery using erythrocytes as carriers," *J. Controlled Release*, vol. 95, no. 1, pp. 27–49, 2004.

[46] C.-M. J. Hu, L. Zhang, S. Aryal, C. Cheung, R. H. Fang, and L. Zhang, "Erythrocyte membrane-camouflaged polymeric nanoparticles as a biomimetic delivery platform," *Proc. Natl. Acad. Sci.*, vol. 108, no. 27, pp. 10980–10985, 2011.

[47] S. Ardekani *et al.*, "Nanoliposomal nitroglycerin exerts potent anti-inflammatory effects," *Sci. Rep.*, vol. 5, p. 16258, 2015.

[48] J. Voigt, J. Christensen, and V. P. Shastri, “Differential uptake of nanoparticles by endothelial cells through polyelectrolytes with affinity for caveolae,” *Proc. Natl. Acad. Sci.*, vol. 111, no. 8, pp. 2942–2947, 2014.